Compressive Yield Stress from Multiple-Speed Centrifuge Measurements

Y. Leong Yeow
Dept. of Chemical Engineering, University of Melbourne, Melbourne, Victoria 3010, Australia

Yee Kwong Leong
School of Engineering, James Cook University, Townsville, Queensland 4811, Australia

Multiple-speed centrifuge measurement is a standard technique for obtaining the compressive yield stress of concentrated suspensions. Converting the centrifuge data into a compressive yield stress vs. volume fraction curve is an inverse problem. The problem is ill posed in the sense that noise in the data is likely to be amplified if inappropriate data processing methods are used. A method based on Tikhonov regularization is applied to solve this inverse problem. An added complication of centrifuge measurement is the interface between the uncompressed and compressed layers in the centrifuge tube. This interface is not measured and has to be treated as a free boundary. A computation scheme for locating this free boundary is incorporated into the Tikhonov regularization procedure. This new way of processing centrifuge data is assessed by applying it to synthetic data and to laboratory data. Problems caused by small or noisy data sets are discussed.

Introduction

A frequently encountered step in the processing of mineral and colloidal suspensions is the dewatering of such suspensions to increase the volume fraction ϕ of solids. Dewatering can be carried out, for example, in thickeners or filter presses. One of the key material properties that controls the extent to which dewatering of a suspension can be achieved is its compressive yield stress p_Y (Buscall and White, 1987). It is a measure of the strength of the structure formed by the solids in the suspension. p_Y normally increases monotonically with ϕ. There are a number of experimental methods for the determination of the compressive yield stress as a function of volume fraction $p_Y(\phi)$. These include the multiple-speed centrifuge measurement (Buscall, 1982; Buscall and White, 1987), the centrifuge concentration profile method (Bergström et al., 1992), and the constant pressure filtration test (Miller et al., 1996; Green et al., 1998). Green and Boger (1997) compared the performance of these methods. The present investigation is concerned with the treatment of the experimental data generated by multiple-speed centrifuge measurement.

Correspondence concerning this article should be addressed to Y. L. Yeow.

Buscall (1982) and Buscall and White (1987) derived the governing equations of dewatering in centrifuges. Their equations are in terms of particle pressure p, compressive yield stress p_Y, and volume fraction ϕ. These authors also outlined the key steps and some of the approximations that can be made for extracting the material property function $p_Y(\phi)$ from centrifuge data. More recently, Green et al. (1996) described a computational procedure for doing this. Their procedure requires the differentiation of the experimental data. This can be taken as an indication that extracting $p_Y(\phi)$ from centrifuge data is an inverse problem and is ill posed in the sense that results are very sensitive to the noise in the data (Engl et al., 2000). The findings of Green et al. (1996) have confirmed this.

There is a group of numerical methods, often referred to by the general name regularization methods (Engl et al., 2000), that are designed specifically for ill-posed inverse problems. These methods are more effective than conventional methods in coping with the unavoidable noise in experimental data. This has motivated the re-examination of the problem of extracting $p_Y(\phi)$ from the centrifuge data with regularization methods in mind. In this article the problem of

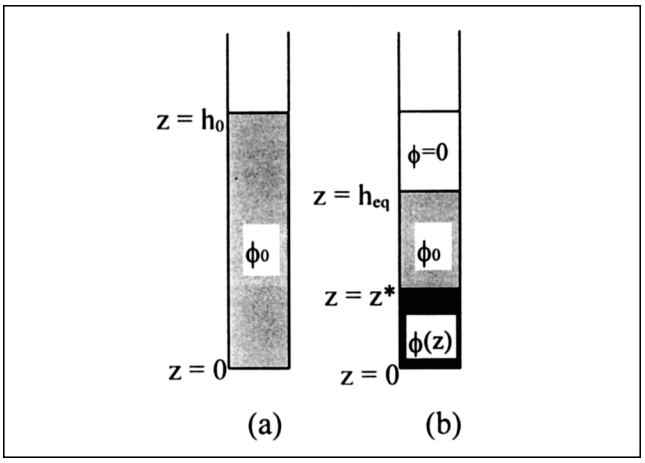

Figure 1. Separation in a centrifuge tube.
(a) Initial condition; (b) at equilibrium.

solving for $p_Y(\phi)$ is first reduced to one of finding the solution of a Volterra integral equation of the first kind. This equation reveals explicitly the inverse and ill-posed nature of the problem. Tikhonov regularization (Engl et al., 2000) is then used to extract $p_Y(\phi)$ from the centrifuge data. Since the ill-posed nature of the problem has been taken into consideration there are good reasons to expect the resulting $p_Y(\phi)$ to be more reliable. Furthermore, as Tikhonov regularization does not involve differentiation of experimental data, it has the added advantage of simplifying the computational steps.

In multiple-speed centrifuge measurement, the centrifuge tube is filled to a height of h_0 with the suspension under investigation. The initial volume fraction of solids of the suspension is denoted by ϕ_0. See Figure 1. The centrifuge is spun at a series of increasing speeds. At any rotational speed, after equilibrium has been reached, the contents in the tube separate into three zones. Topmost in the tube is a layer of clear supernatant liquid. Below this is a layer of uncompressed solids at the original volume fraction ϕ_0. This is followed by a layer of compressed solids where the volume fraction $\phi(z)$ increases towards the bottom of the tube (Buscall and White, 1987). In normal centrifuge measurement, the location of the interface between the supernatant liquid and the uncompressed zone h_{eq} is measured, but that between the uncompressed and compressed solid layers z^* is not. It is necessary to know the exact location of this second interface in order to compute the $p_Y(\phi)$ curve. This second interface thus becomes a free boundary of the problem and has to be determined during the solution of the integral equation of the first kind. For this purpose, a computational scheme with the unknown compressive yield stress p_0 at the initial volume fraction ϕ_0 as the free parameter has been developed. This scheme is incorporated into the Tikhonov regularization computation to determine $p_Y(\phi)$. The L-curve method (Engl et al., 2000) is then applied to select the most appropriate value of p_0.

To assess its performance, the procedure based on Tikhonov regularization is first applied to solve the inverse problem of centrifuge measurement with synthetic data. Gaussian noise is imposed on these data to test the effectiveness of Tikhonov regularization in noise handling. Testing with synthetic data also allows the effects of the regularization parameter introduced by Tikhonov regularization on the final $p_Y(\phi)$ curve to be investigated. Tikhonov regularization is then used to process a typical set of laboratory data taken from the recent literature. Centrifuge data sets are often very small and may have relatively high noise level. For such cases, direct application of Tikhonov regularization may not result in a physically meaningful $p_Y(\phi)$ curve. To deal with these difficult situations, augmenting the data set and/or pre-filtering the experimental noise are investigated.

Centrifuge Measurement and the Governing Equations

Experimental data

In multiple-speed centrifuge measurement, the experimental results take the form of a set of equilibrium heights h_{eq} vs. rotational speeds ω, or equivalently, centrifugal accelerations g data points: $(h_{\text{eq1}}, g_1), (h_{\text{eq2}}, g_2), (h_{\text{eq3}}, g_3) \ldots (h_{\text{eq}N_D}, g_{N_D} = g_{\max})$. N_D is the number of data points. In many practical situations N_D can be as small as 5 to 10. g_i, the acceleration at the base of the centrifugal tube for the ith data point, is related to the corresponding rotational speed ω_i by $g_i = \omega_i^2 R$. R is the distance between the base of the tube and center of the centrifuge. Other experimental data needed in the computation of the compressive yield stress are the density difference $\Delta\rho$ between the suspended solid and the suspending liquid, the uniform volume fraction of solids ϕ_0 in the original suspension and the corresponding initial height of the suspension h_0. The compressive yield stress p_0 at ϕ_0 is generally not known beforehand. (p_0, ϕ_0) forms the lower endpoint of the required $p_Y(\phi)$ curve. Experimental details of multiple-speed centrifuge measurement can be found in Buscall (1982).

Governing equations

At equilibrium, the particle pressure $p(z)$ and volume fraction $\phi(z)$, in both the uncompressed and compressed layers, are related by (Buscall and White, 1987)

$$\frac{dp}{dz} = -\phi g \Delta\rho \left(1 - \frac{z}{R}\right). \tag{1}$$

Equation 1 is the result of force balance. The z coordinate is in the opposite direction to g. $z = 0$ (see Figure 1) is the base of the centrifuge tube. In the compressed layer $p(z)$ is the compressive yield stress $p_Y(z)$ at the corresponding local volume fraction $\phi(z)$. The subscript Y for compressive yield stress will be omitted except in situations where an omission may lead to ambiguity. In the uncompressed solid layer the particle pressure generated by centrifugal acceleration is insufficient to bring about any dewatering. Consequently ϕ remains constant at ϕ_0 throughout this layer.

The two unknowns of the inverse problem of centrifuge measurement are p and ϕ as a function of height z. A sec-

ond equation is needed. This is provided by material balance

$$\int_{z=0}^{h_{eq}} \phi(z)dz = \int_{z=0}^{z^*} \phi(z)dz + \int_{z^*}^{h_{eq}} \phi(z)dz$$
$$= \int_{z=0}^{z^*} \phi(z)dz + (h_{eq} - z^*)\phi_0$$
$$= h_0\phi_0. \quad (2)$$

z^* is the location of the free boundary between the compressed and uncompressed layers. Between $z^* < z < h_{eq}$, the suspension is in its original uncompressed state with volume fraction ϕ_0. z^* is, as mentioned above, not normally measured.

Boundary conditions

At the interface between the uncompressed layer and the supernatant liquid

$$z = h_{eq}, \phi = \phi_0 \text{ and } p = 0. \quad (3)$$

At the free boundary between the compressed and uncompressed layers

$$z = z^*, \phi = \phi_0 \text{ and } p = p_0. \quad (4)$$

ϕ_0 is known, but p_0 is not.

Equations 1–4 form the starting point of the present investigation. They are also the equations used by Green et al. (1996) in their computation. For a discussion of the physical assumptions that led to this set of equations and boundary conditions, see Buscall (1982) and Buscall and White (1987).

Dimensionless Variables and Equations

To ensure generality of the computational scheme to be developed, the following scaling factors are introduced: reference length = R, reference volume fraction = ϕ_0, reference acceleration = $g_{N_D} = g_{max}$, and reference stress = $\Delta\rho g_{max} R\phi_0$. Based on these factors, the following dimensionless variables follow naturally: $Z = z/R$, $H_{eq} = h_{eq}/R$, $Z^* = z^*/R$, $\Phi = \phi/\phi_0$, $G = g/g_{max}$, and $P = p/(\Delta\rho g_{max} R\phi_0)$. The physical meaning of these dimensionless variables are self-evident. In dimensionless form, the empirical data become (H_{eq1}, G_1), (H_{eq2}, G_2), $(H_{eq3}, G_3)\ldots(H_{eqN_D}, G_{N_D} = 1)$. The dimensionless initial height will be denoted by $H_0 = h_0/R$. H_0 is also the total amount of solid in the sample in dimensionless terms. The dimensionless equivalent of the unknown initial compressive yield stress p_0 will be denoted by $P_0 = p_0/(\Delta\rho g_{max} R\phi_0)$.

The dimensionless governing equations are

$$\frac{dP}{dZ} = -\Phi G(1 - Z), \quad (5)$$

$$\int_{Z=0}^{Z^*} \Phi(Z)dZ + (H_{eq} - Z^*) = H_0. \quad (6)$$

In dimensionless form, boundary conditions 3 and 4 become

$$Z = H_{eq}, \Phi = 1 \text{ and } P = 0 \quad (7)$$

and

$$Z = Z^*, \Phi = 1 \text{ and } P = P_0 \quad (8)$$

respectively. The form of Eq. 5 suggests the introduction of an alternative independent variable Y defined by

$$Y = \left(Z - \frac{Z^2}{2}\right)G. \quad (9)$$

Expressions giving Z and its first derivative in terms of Y, needed in the subsequent computation, follow directly from Eq. 9

$$Z = 1 - \sqrt{1 - \frac{2Y}{G}}, \quad (10)$$

and

$$\frac{dZ}{dY} = \frac{1}{\sqrt{G}\sqrt{G - 2Y}}. \quad (11)$$

In terms of Y, Eq. 5 reduces to

$$\frac{dP[\Phi(Y)]}{dY} = -\Phi(Y). \quad (12)$$

Boundary conditions 7 and 8 now take the form

$$Y = Y_{eq}, \phi = 1 \text{ and } P = 0 \quad (13)$$

and

$$Y = Y^*, \Phi = 1 \text{ and } P = P_0 \quad (14)$$

respectively.

In the uncompressed layer $\Phi = 1$, Eq. 12 simplifies to

$$\frac{dP(\Phi(Y))}{dY} = -1$$

This can be integrated and combined with the boundary condition 13 to give $P(Y) = Y_{eq} - Y$. Imposing boundary condition 14 leads to $P_0 = P(Y^*) = Y_{eq} - Y^*$, that is

$$Y^* = Y_{eq} - P_0. \quad (15)$$

This last relationship gives Y^* in terms of the experimentally measured H_{eq} (and, hence, Y_{eq}) and the unknown P_0. Z^* can in turn be obtained from Y^* using Eq. 10.

Integral Equation of the First Kind

Treating P as a function of Φ, Eq. 12 can, in principle, be integrated across the compressed layer to give Φ as a function of Y. This function will be denoted by $F(Y)$. According to boundary condition 14, at the free boundary, $\Phi = 1$ when $Y = Y^*$. The value of Y^* is not known and changes with the G of each of the experimental data points. The general solution for $\Phi(Y)$ can be written as

$$\Phi(Y) = F(Y^* - Y), \tag{16}$$

with the understanding that $F(0) = 1$. Substituting Eq. 16 into Eq. 6 and changing the variable of the integration from Z to Y gives

$$\int_{Y=0}^{Y^*} F(Y^* - Y)\left(\frac{1}{\sqrt{G}\sqrt{G - 2Y}}\right) dY = H_0 - (H_{\text{eq}} - Z^*). \tag{17}$$

Making a further change of variable $\chi = Y^* - Y$, Eq. 17 reduces to

$$\int_{\chi=0}^{\chi=Y^*} F(\chi)\left(\frac{1}{\sqrt{G}\sqrt{G - 2(Y^* - \chi)}}\right) d\chi = H_0 - (H_{\text{eq}} - Z^*). \tag{18}$$

The righthand side of this equation represents the amount of solids, in dimensionless terms, that resides in the compressed layer when equilibrium has been reached. It can be evaluated for each of the experimental data points (G_i, $H_{\text{eq}i}$) using an assumed value of the free parameter P_0 (after using Eqs. 15 and 10 to obtain Y^* and Z^*, respectively). This quantity will be denoted by Q_i^M, $i = 1,2,\ldots N_D$. Superscript M is used here as a reminder that these are experimentally measured quantities. Equation 18 can now be regarded as an integral equation for the unknown function $F(\chi)$ for the assumed value of P_0. It is in the form of a Volterra integral equation of the first kind that is known to be ill posed (Engl et al., 2000).

In discretized form the lefthand side of Eq. 18 becomes

$$Q_i^C = \sum_{\chi_j = \chi_1 = 0}^{Y_i^*} \frac{\alpha_{ij} F_j \Delta\chi}{\sqrt{G_i}\sqrt{G_i - 2(Y_i^* - \chi_j)}}, \quad i = 1,2,\ldots,N_D. \tag{19}$$

Q_i^C is the computed equivalent of Q_i^M. χ_j, for $j = 1, 2,\ldots N_K$, are the discretization points of the independent variable $0 \le \chi \le Y_{N_D}^*$ and $\Delta\chi$ is the step size. F_j is the discretized $F(\chi)$ at χ_j. α_{ij} is the coefficient arising from the numerical scheme used to approximate the integral in Eq. 18. For example, for Simpson's 1/3 rule, $\alpha_{ij} = 2/3$ when j is odd and 4/3 when jth is even. Depending on whether the Y_i^* associated with the ith experimental data point coincides with a discretization point, the last α_{ij} associated with this point may have to be adjusted, by interpolation, to allow for fractional step size.

The deviation of Q_i^C from Q_i^M, expressed as a fraction of the total solids in the sample, is

$$\delta_i = \frac{Q_i^M - \sum_{\chi_j = \chi_1 = 0}^{Y_i^*} \frac{\alpha_{ij} F_j \Delta\chi}{\sqrt{G_i}\sqrt{G_i - 2(Y_i^* - \chi_j)}}}{H_0} = \frac{Q_i^M}{H_0} - \sum_{j=1}^{Y_i^*} A_{ij} F_j \tag{20}$$

or, in matrix notation, $\boldsymbol{\delta} = \boldsymbol{Q}^M/H_0 - \boldsymbol{AF}$. $\boldsymbol{Q}^M$ is the $N_D \times 1$ column vector of Q_i^M and $\boldsymbol{A}$ is the $N_D \times N_K$ matrix of coefficients of the unknown column vector $\boldsymbol{F}$. $\boldsymbol{A}$ is given by

$$A_{ij} = \frac{\frac{\alpha_{ij}\Delta\chi}{\sqrt{G_i}\sqrt{G_i - 2(Y_i^* - \chi_j)}}}{H_0}, \quad i = 1,2,3\ldots N_D, \quad j = 1,2,3\ldots N_K. \tag{21}$$

As the number of discretization points N_K is larger than the number of data points N_D, $\boldsymbol{A}$ is not a square matrix and cannot be inverted to give a unique $\boldsymbol{F}$. Instead $\boldsymbol{F}$ is selected to minimize the sum of squares of δ_i, that is, to minimize

$$\sum_{i=1}^{N_D} \delta_i^2 = \underline{\boldsymbol{\delta}}^T\underline{\boldsymbol{\delta}} = \left(\frac{\boldsymbol{Q}^M}{H_0} - \boldsymbol{AF}\right)^T\left(\frac{\boldsymbol{Q}^M}{H_0} - \mathbf{AF}\right) = \left(\frac{\boldsymbol{Q}^M}{H_0}\right)^T\left(\frac{\boldsymbol{Q}^M}{H_0}\right) - 2\boldsymbol{F}^T\boldsymbol{A}^T\left(\frac{\boldsymbol{Q}^M}{H_0}\right) + \boldsymbol{F}^T\boldsymbol{A}^T\boldsymbol{AF}^T \tag{22}$$

It is worth pointing out that in many applications of Tikhonov regularization, instead of minimizing the fractional deviation defined in Eq. 20, the absolute deviation between the computed variable and its experimentally measured counterpart is minimized. See, for example, Weese (1992). Using fractional deviation in preference to absolute deviation, as in the present investigation, means that the data points at high and low G are weighted equally.

Tikhonov Regularization

Because of the noise in the experimental data, minimizing $\underline{\boldsymbol{\delta}}^T\underline{\boldsymbol{\delta}}$ will not in general result in a smooth $F(\chi)$ (Engl et al., 2000). To ensure a smooth $F(\chi)$, additional conditions, regularization conditions, have to be imposed. In the present investigation, the additional condition is the minimization of the sum of squares of the second derivative $d^2F/d\chi^2$ at the internal discretization points. In terms of the column vector $\boldsymbol{F}$, this condition takes on the form of minimizing

$$\sum_{j=2}^{N_K - 1}\left(\frac{d^2F}{d\chi^2}\right)_j^2 = (\underline{\boldsymbol{\beta}}\boldsymbol{F})^T(\underline{\boldsymbol{\beta}}\boldsymbol{F}) = \boldsymbol{F}^T\underline{\boldsymbol{\beta}}^T\underline{\boldsymbol{\beta}}\boldsymbol{F} \tag{23}$$

where $\boldsymbol{\beta}$ is the tri-diagonal matrix of coefficients arising from the finite difference approximation of $d^2F/d\chi^2$

$$\underline{\boldsymbol{\beta}} = \begin{bmatrix} 1 & -2 & 1 & & & & \\ & 1 & -2 & 1 & & & \\ & & 1 & -2 & 1 & & \\ . & . & . & . & . & . & . \\ . & . & . & . & . & . & . \\ & & & 1 & -2 & 1 & \\ & & & & 1 & -2 & 1 \end{bmatrix} \frac{1}{(\Delta\chi)^2}. \quad (24)$$

In Tikhonov regularization (Engl et al., 2000) instead of minimizing $\underline{\boldsymbol{\delta}}^T\underline{\boldsymbol{\delta}}$ and $\boldsymbol{F}^T\underline{\boldsymbol{\beta}}^T\boldsymbol{F}$ separately, a linear combination of these two quantities $R = \underline{\boldsymbol{\delta}}^T\underline{\boldsymbol{\delta}} + \lambda\boldsymbol{F}^T\underline{\boldsymbol{\beta}}^T\underline{\boldsymbol{\beta}}\boldsymbol{F}$ is minimized. λ is an adjustable positive weighting factor that controls the extent to which the noise in the experimental data is being filtered out. It balances the two requirements on $F(\chi)$: (i) fitting the centrifuge data and (ii) remaining as smooth as possible. A large λ will give a smooth $F(\chi)$, but at the expense of the goodness of fit of the experimental data. The most appropriate value of λ depends on factors such as the noise level in the experimental data, the number of data points N_D, and discretization points N_K, and the numerical schemes used to approximate the integral in Eq. 18 and the second derivative in Eq. 23. It is neither a property of the material under test, nor a parameter of the apparatus used in the measurement.

Minimizing R requires

$$\frac{\partial R}{\partial F_j} = 0, \quad j = 1,2,\ldots N_K \quad (25)$$

This gives a set of linear algebraic equations for $\boldsymbol{F}$. It can be shown (Shaw and Tigg, 1994) that the $\boldsymbol{F}$ which satisfies Eq. 25 is given by

$$\boldsymbol{F} = \left(\boldsymbol{A}^T\boldsymbol{A} + \lambda\underline{\boldsymbol{\beta}}^T\underline{\boldsymbol{\beta}}\right)^{-1}\boldsymbol{A}^T\left(\frac{\boldsymbol{Q}^{\boldsymbol{M}}}{H_0}\right). \quad (26)$$

This is the "solution" to the Volterra integral equation, Eq. 18, given by Tikhonov regularization.

Algebraic Equation Relating λ and p_0

In normal Tikhonov regularization computation λ is a parameter that can be freely adjusted. However, because of the unknown free boundary between the compressed and uncompressed layers, λ is not a free parameter in the inverse problem of centrifuge measurement. Instead, λ depends on the assumed value of p_0 (or, equivalently, P_0). The equation relating λ to p_0 will now be developed.

From the way it was obtained, it can be seen that the solution given by Eq. 26 depends on P_0 and λ. This dependence will be made explicit by denoting the solution as $F(\chi, P_0, \lambda)$. In terms of this solution the boundary condition 14 becomes

$$F(\chi = 0, P_0, \lambda) = 1. \quad (27)$$

This equation can be regarded as a nonlinear algebraic equation relating P_0 and λ. For any appropriately specified P_0, the associated positive λ is found by solving Eq. 27 using standard Newton-Raphson procedure.

However, it should be noted that, depending on the size of and the noise level in a data set, there may not be a combination of $(P_0 > 0,\ \lambda > 0)$ that satisfies Eq. 27. Also, the compressive yield stress curves associated with the physically meaningful solutions (P_0, λ) of Eq. 27 may not be sufficiently smooth and monotonic. In such events it was found that by increasing the number of data points N_D or reducing the noise level by pre-filtering will often overcome the problem. This will be demonstrated by the two case studies presented below.

From the above description, it can be seen that for the inverse problem of centrifuge measurement the free regularization parameter λ has been replaced by the free physical parameter p_0. The outcome of the Tikhonov regularization computation is thus not a single solution, but a family of solutions of Eq. 27 each associated with a particular combination of $(P_{01},\ \lambda_1)$, $(P_{02},\ \lambda_2)$, $(P_{03},\ \lambda_3)\ldots$. A method based on the L-curve (Engl et al., 2000) will be used to select the most appropriate value for P_0 from all the possible $(P_0,\ \lambda)$ combinations. Details of the L-curve method will be described in the Discussion section with reference to a specific example.

With an appropriate P_0 and the resulting $F(\chi)$ provided by Tikhonov regularization, Eq. 12 together with the boundary condition 14 in the form $P(\chi = 0) = P_0$ can now be integrated numerically, by standard Runge-Kutta procedure, to give $P(\chi)$. Finally, the required dimensionless volume fraction vs. compressive yield stress relationship $P(\Phi)$ is obtained by combining $\Phi(\chi)$ and $P(\chi)$. Provided the $F(\chi)$ generated by Tikhonov regularization is smooth and monotonic, the resulting compressive yield stress vs. volume fraction curve will also be smooth and monotonic.

Data and Results

(a) Synthetic data and results

Following Green et al. (1996), the power-law equation

$$p_Y(\phi) = 100\left[\left(\frac{\phi}{0.18}\right)^8 - 1\right] \quad (28)$$

was used to generate a set of eight synthetic h_{eq} vs. g data points. The relevant experimental conditions, taken from Green et al. (1996), are: $h_0 = 0.0885$ m, $\Delta\rho = 1{,}212$ kg·m^{-3}, $R = 0.1558$ m, and $\phi_0 = 0.194$. To simulate experimental noise, Gaussian noise with zero mean and standard deviation of 5% was added to the synthetic data generated by Eq. 28. The resulting "noisy" data are shown in Figure 2 as open squares. This level of random noise should be compared against the 2% noise imposed by Green et al. (1996). The purpose of introducing this relatively high level of noise is to push the Tikhonov regularization procedure beyond its limits and to investigate possible remedies when the procedure fails.

Green et al. (1996) has shown that, when the noise level is high, direct processing of the centrifuge data does not lead to physically sensible results. To overcome this problem, they pre-filtered the data prior to processing. Tikhonov regularization is able to cope directly with the synthetic data from

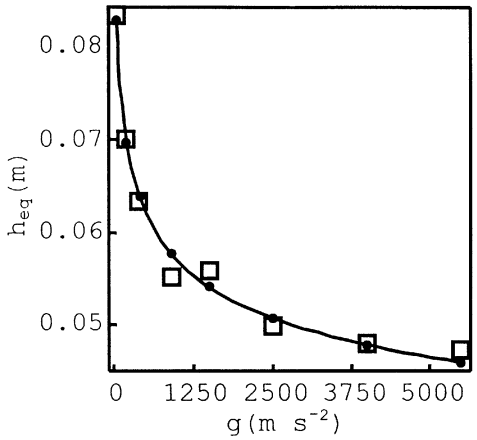

Figure 2. Simulated centrifuge data.

Open squares are data with 5% imposed noise and filled circles are pre-filtered data.

Eq. 28 with 2% imposed noise, but fails when the noise level is increased to 5% and beyond, that is, the resulting compressive yield stress curves are not physically acceptable. Prefiltering of the noise becomes necessary. In the present investigation pre-filtering is achieved by fitting a curve of the simple form

$$h_{\text{eq}}(g) = kg^m \tag{29}$$

through the noisy data points. k and m are constants determined by least-squares fitting. The filled circles in Figure 2 are the pre-filtered data and the curve going through these data points is Eq. 29. The form of Eq. 29, suggested by Buscall and White (1987), is based on the empirical observation that, on a log-log plot, centrifuge data points are very close to linear. It is the simplest curve that can fit the data satisfactorily.

The $p_Y(\phi)$ relationship obtained by Tikhonov regularization from the pre-filtered data is shown in Figure 3. The discrete points on this plot are the results of Tikhonov computation and the continuous curve is the original power-law Eq. 28. In arriving at this $p_Y(\phi)$, different p_0 and its associated λ were tested out. The final choice is $p_0 = 90.27$ Pa. See Discussion below.

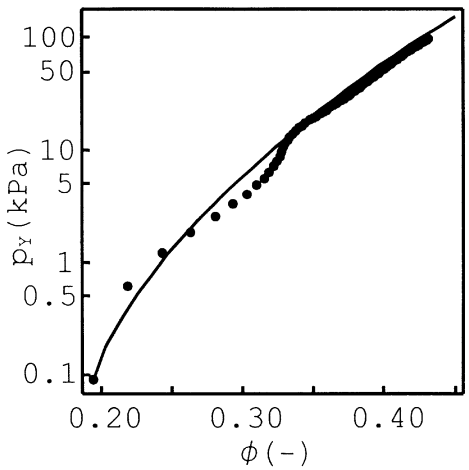

Figure 3. Compressive yield stress curve.

The continuous curve is Eq. 28 and the discrete points are by Tikhonov regularization.

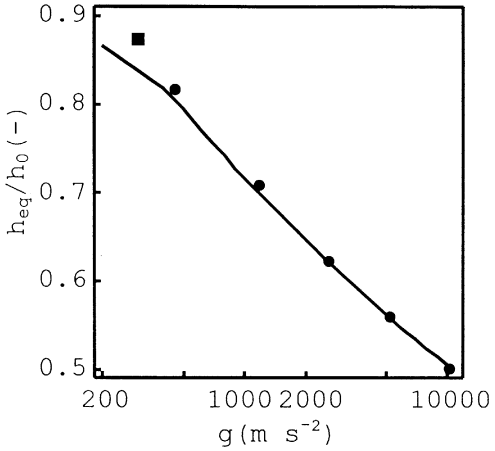

Figure 4. h_{eq}/h_0 vs. g data for the ZrO_2 suspension.

Filled circles are experimental data (Green and Boger, 1997) and the filled square is by Eq. 29. The curve is based on the results of Tikhonov regularization.

(b) Zirconium dioxide ZrO_2 suspension

In their evaluation of the various methods of measuring compressive yield stress, Green and Boger (1997) published several sets of experimental multiple-speed centrifuge data. A typical set is reproduced here in Figure 4 as filled circles. These data are for an aqueous suspension of zirconium dioxide ZrO_2 ($\rho = 5{,}720$ kg·m^{-3}) at pH of 7.1. The initial volume fraction is $\phi_0 = 0.15$ and the initial height $h_0 = 0.0925$ m. The distance to the base of the centrifuge tube is $R = 0.149$ m. These experimental conditions were taken from Green and Boger (1997) and supplemented by data from Green (1997).

It was found that, with the original 5-point data set, Eq. 27 does not have a physically meaningful solution, that is, one where $P_0 > 0$ and $\lambda > 0$. A least-squares curve, not shown, of the form in Eq. 29 was fitted through the filled circles in Figure 4 to filter out the experimental noise and to generate an extra data point at $g = 300$ m·s^{-2}. This extra point is shown as a filled square in this figure. The six data points in Figure 4 are treated as a combined set in Tikhonov regularization.

The $p_Y(\phi)$ obtained by Tikhonov regularization for this ZrO_2 suspension is shown in Figure 5 as a continuous curve. The volume fraction covered by this curve is from the initial volume fraction of 0.15 to just over 0.35. To arrive at this curve, different p_0 and the associated λ were again investigated. For the curve in Figure 5, $p_0 =$ 649.93 Pa (see below). The discrete points in Figure 5 are the results of Green and Boger (1997), which are included here for comparison. Their results are based only on the five original experimental data points in Figure 4.

Discussion

For most suspensions $p_Y(\phi)$, is a positive, smooth, and monotonically increasing function. In all the cases investi-

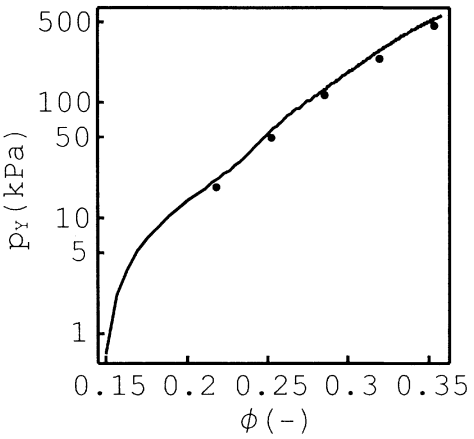

Figure 5. Compressive yield stress vs. volume fraction for ZrO_2 suspension.

The curve is by Tikhonov regularization and the discrete points are from Green and Boger (1997).

gated the results of Tikhonov regularization meet all these physical requirements. However, as shown by the two case studies, the centrifuge data may have to be pre-filtered or augmented if the Tikhonov regularization procedure developed here is to function properly, that is, so that Eq. 27 has acceptable solutions for a sufficiently wide range of p_0.

Pre-filtering is necessary because the $p_Y(\phi)$ curve is very sensitive to the noise in the experimental data. For example, if the noisy data set in Figure 2, denoted by the open squares, is used directly in the Tikhonov regularization procedure, the resulting $p_Y(\phi)$ is not monotonic for all the combinations of $p_0 > 0$ and $\lambda > 0$ that satisfy Eq. 27. Numerical experimentation showed that this difficulty can be overcome by pre-filtering the data using the simple Eq. 29.

In their investigation Green et al. (1996) used different polynomial curves to filter out noise. They found that their result is very sensitive to the functional form of the curve assumed. This is because a key step in their method of obtaining $p_Y(\phi)$ requires the slope of the $h_{eq}(g)$ vs. g curve. They obtained this by evaluating the derivatives at selected points of the fitted least-squares curve. The procedure based on Tikhonov regularization does not involve such a noise amplification differentiation step. Equation 29 is only used to filter out noise and, if necessary, to generate an extra (h_{eq}, g) data point. Consequently, the resulting $p_Y(\phi)$ is far less sensitive to the functional form of the curve assumed.

A closely related problem encountered in the treatment of multiple-speed centrifuge data is the extremely small size of the experimental data set. The time and effort required to perform centrifuge measurements rarely permit the gathering of more than 5 to 10 points in a single data set. The ZrO_2 data (Green and Boger, 1997) in Figure 4 with only five points is an example of a small data set. As mentioned above, with this 5-point data set, Eq. 27 does not have an acceptable solution. The physical origin of this problem can be traced to the paucity of data points at sufficiently low g. Such data points are needed to fix the shape of $p_Y(\phi)$ at ϕ close to initial volume fraction ϕ_0. This difficulty was overcome by using Eq. 29 to generate the extra data point at $g = 300$ m·s^{-2}. Buscall and White (1987) discussed the use of such an equation to augment limited experimental data points. A more satisfactory, but more costly, solution is to perform additional centrifuge measurements at low rotational speeds. These extra experimental data points will improve the reliability of the $p_Y(\phi)$ curve at low ϕ.

Green and Boger (1997) were able to obtain the compressive yield stress of the ZrO_2 suspension without resorting to data augmentation. Since their compressive yield stress results do not extend to the neighborhood of ϕ_0 (see Figure 5), they do not have to deal explicitly with Eq. 27 or its equivalent as the boundary condition at the free boundary. This is a possible explanation why data augmentation becomes unnecessary in their investigation.

For the synthetic data in Figure 2, Tikhonov regularization computation has been carried out to generate a family of solutions for p_0 between 0 Pa and 179.07 Pa. It was observed that the λ given by Eq. 27 decreases with p_0 as p_0 increases from 0 to 179.07 Pa. For $p_0 > 179.07$ Pa, Eq. 27 does not have a positive solution for λ. Thus, the family of solutions provided by Tikhonov regularization is restricted to $0 < p_0 < 179.07$ Pa. Solutions outside this range do not have any physical meaning.

To arrive at a unique $p_Y(\phi)$, the L-curve method (Hansen, 1992) is used to select the most appropriate p_0 from within the range $0 < p_0 < 179.07$ Pa. In this procedure the value of $\boldsymbol{\delta}^T\boldsymbol{\delta}$ (a measure of accuracy) is plotted against that of $\boldsymbol{F}^T\underline{\boldsymbol{\beta}}^T\underline{\boldsymbol{\beta}}\boldsymbol{F}$ (a measure of smoothness) for various assumed values of p_0. Such a plot, referred to as the L-curve, for the synthetic data in Figure 2 is shown in Figure 6. The value of p_0, or equivalently the associated λ, appears as the independent parameter that varies along the L-curve. This curve begins with the parameter $p_0 = 0$ Pa at the righthand end of the plot and terminates at $p_0 = 179.07$ Pa on the left where λ approaches zero.

In most inverse problems, the L-curve is presented on a log-log format and takes the shape of an L with a very sharp corner (hence, the name for this procedure). The most appropriate value of the regularization parameter λ (or p_0 in the present problem) is the one at the corner of the L (Hansen, 1992). Normally, the two arms of the L-curve can, in principle, be extended indefinitely by letting λ vary over sev-

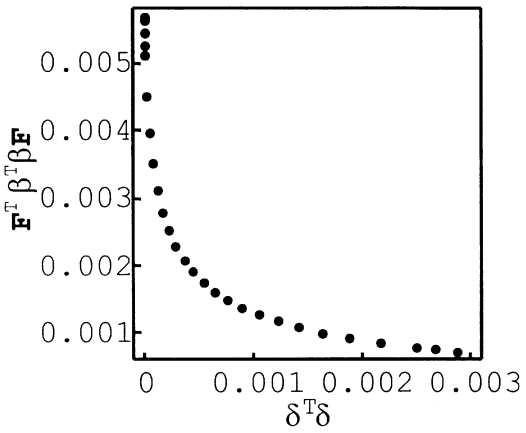

Figure 6. L-curve for the data in Figure 2.

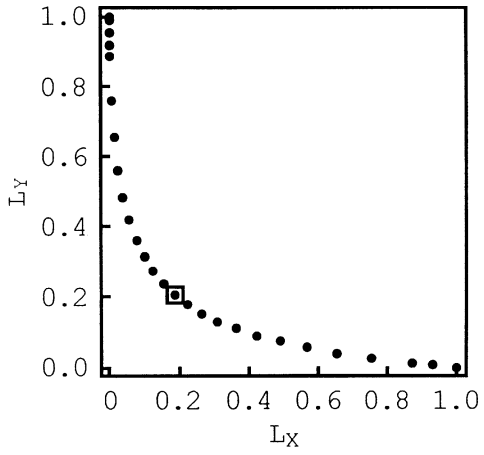

Figure 7. Scaled L-curve for the data in Figure 2.
The open square marks the "corner" of the curve.

eral orders of magnitude. The L-curves arising from centrifuge measurement differ from the normal L-curve in two significant ways. First, as explained above, the L-curve of centrifuge measurement can only be constructed for a finite range of the parameter p_0. Second, the L-curve of this problem does not have a sharp corner. See Figure 6. Consequently, the L-curve does not lead to a well-defined value for the most appropriate p_0.

This lack of a sharp corner can be partially remedied by re-plotting the L-curve in terms of the following scaled coordinates

$$L_{Xi} = \frac{\left(\underline{\boldsymbol{\delta}}^T\underline{\boldsymbol{\delta}}\right)_i - \left(\underline{\boldsymbol{\delta}}^T\underline{\boldsymbol{\delta}}\right)_{\min}}{\left(\underline{\boldsymbol{\delta}}^T\underline{\boldsymbol{\delta}}\right)_{\max} - \left(\underline{\boldsymbol{\delta}}^T\underline{\boldsymbol{\delta}}\right)_{\min}}, \tag{30}$$

$$L_{Yi} = \frac{\left(\boldsymbol{F}^T\underline{\boldsymbol{\beta}}^T\underline{\boldsymbol{\beta}}\boldsymbol{F}\right)_i - \left(\boldsymbol{F}^T\underline{\boldsymbol{\beta}}^T\underline{\boldsymbol{\beta}}\boldsymbol{F}\right)_{\min}}{\left(\boldsymbol{F}^T\underline{\boldsymbol{\beta}}^T\underline{\boldsymbol{\beta}}\boldsymbol{F}\right)_{\max} - \left(\boldsymbol{F}^T\underline{\boldsymbol{\beta}}^T\underline{\boldsymbol{\beta}}\boldsymbol{F}\right)_{\min}} \tag{31}$$

for the set of points p_{01}, p_{02}, p_{03},... p_{0i}... in Figure 6. Figure 7 is the scaled equivalent of Figure 6. Because of the way they are defined, the scaled coordinates L_{Xi} and L_{Yi} both lie between 0 and 1. The scaled L-curve is more symmetrical about the diagonal line $L_X = L_Y$. The "corner" is now taken to be the neighborhood of the intersection of the scaled L-curve with this diagonal line. This "corner" is marked by the open square in Figure 7. The value of p_0 at this point is 90.27 Pa. This is the value used to generate the computed $p_Y(\phi)$ curve in Figure 3. Numerical experimentation reveals that small changes in p_0 about the "corner" only affects $p_Y(\phi)$ at low ϕ. The $p_Y(\phi)$ curve for large ϕ is not significantly affected.

This modified L-curve method was also used to locate the value of p_0 for the ZrO_2 suspension. In this case at the "corner" of the curve $p_0 = 649.93$ Pa. This is the p_0 for the $p_Y(\phi)$ in Figure 5. The range of p_0 over which the L-curve can be constructed is $0 < p_0 < 1134.52$ Pa.

A number of checks have been performed on the results of Tikhonov regularization. Figure 3 shows a comparison of the computed $p_Y(\phi)$ against the original power-law Eq. 28. Tikhonov regularization clearly has been able to reproduce the original $p_Y(\phi)$ curve to a high degree of accuracy at high volume fraction ϕ even in the presence of the 5% imposed random noise. Because of the noise in the synthetic data, the computed $p_Y(\phi)$ curve is not very smooth. However, it satisfies the positive monotonic increasing requirement. Numerical experimentation shows that as the noise level is reduced, not only does the resulting curve become smoother it also approaches the theoretical Eq. 28 over the entire range of ϕ. When the noise is sufficiently low, Tikhonov regularization can be applied to the noisy data directly without having to go through the least-squares pre-filtering step.

More significantly, comparison with the original power-law equation shows that the modified L-curve method has selected a p_0 of 90.27 Pa, which is approximately 10% above the theoretical value of 82.07 Pa. As the noise level is reduced or when additional low centrifuge speed data are available, numerical results show that the modified L-curve method will converge on a more accurate p_0 and this is accompanied by improvements in the computed $p_Y(\phi)$ curve.

Figure 5 shows that, at higher volume fractions, the computed $p_Y(\phi)$ curve is in very good agreement with the discrete results of Green and Boger (1997). In view of the fundamentally different approach adopted by Green et al. (1996) compared to that of the present investigation, this level of agreement is quite unexpected.

For the ZrO_2 suspension, the modified L-curve procedure gave a p_0 of 649.93 Pa. This value appears to be physically reasonable, but there is no available experimental data to verify its accuracy. It is, however, of the correct magnitude when compared to some of the $p_Y(\phi)$ curves in Green (1997) for various ZrO_2 suspensions under similar conditions. The lack of sharpness of the scaled L-curve means that the value of p_0 cannot, in general, be determined to an accuracy better than approximately $\pm 10\%$. As with the synthetic data, the reliability of the computed $p_Y(\phi)$ at low ϕ for the ZrO_2 suspension can be greatly improved if additional low g data points are available.

Most existing methods of obtaining $p_Y(\phi)$ require an extensive amount of iterative curve fitting and numerical differentiation. As a consequence, these methods normally only compute the compressive yield stress at a small number of discrete ϕ. An obvious advantage of Tikhonov regularization is that it generates an entire $p_Y(\phi)$ curve, for $\phi_0 \le \phi \le \phi_{\max}$ where $\phi_{\max}$ is the highest volume fraction of solids attained in the centrifuge data set. This represents the maximum amount of information that can be extracted from the data set.

It is also worth noting that existing methods of obtaining $p_Y(\phi)$ usually do not permit the computation of the compressive yield stress close to ϕ_0. See, for example, the results of Green and Boger (1997) in Figure 5. The Tikhonov regularization procedure developed here, because it incorporates the condition at the free boundary at z^*, is able to obtain $p_Y(\phi)$ in the neighborhood of ϕ_0 where the curve is highly nonlinear and, hence, less predictable. The shape of the $p_Y(\phi)$ curve in this region is of some practical importance as it characterizes the behavior, during the initial stages, of any dewatering process.

As a final check, the computed $p_Y(\phi)$ in Figure 5 was used to compute the complete equilibrium height vs. rotational speed curve for the experimental conditions in question. The computed $h_{eq}(g)$ curve is shown in Figure 4. Apart from the single point at the lowest rotational speed, the computed result is in very good agreement with the experimental data of Green and Boger (1997). Since the computer program used to solve for $h_{eq}(g)$, the direct problem, is completely independent of the Tikhonov regularization program for the inverse problem, this agreement can be regarded as an independent validation of the results of Tikhonov regularization computation.

Conclusion

The problem of extracting the $p_Y(\phi)$ relationship from the multiple-speed centrifuge data of a suspension has been formulated as an integral equation of the first kind. It has also been demonstrated that Tikhonov regularization is an effective and relatively simple method for solving this inverse problem. The L-curve provides a suitable means of locating the compressive yield stress at the initial volume fraction of the suspension. For a noisy or small data set, it may be necessary to pre-filter the noise or to augment the data at low rotational speeds.

Acknowledgment

YLY thanks Dr. Ross de Kretser of the Particulate Fluids Processing Centre, Dept. of Chemical Engineering, University of Melbourne for advice regarding the experimental data on the ZrO_2 suspension. This work was supported by the Melbourne Research Development Grant Scheme.

Literature Cited

Bergström, L., C. H. Schilling, and I. A. Aksay, "Consolidation Behavior of Flocculated Alumina Suspensions," *J. Amer. Ceram. Soc.*, **75**, 3305 (1992).

Buscall, R., "The Elastic Properties of Structured Dispersions: A Simple Centrifuge Method of Examination," *Colliods Surf.*, **5**, 269 (1982).

Buscall, R., and L. R. White, "The Consolidation of Concentrated Suspensions: 1. The Theory of Sedimentation," *J Chem. Soc., Farad. Trans. 1*, **83**, 873 (1987).

Engl, H. W., M. Hanke, and A. Neubauer, *Regularization of Inverse Problems*, Kluwer, Dordrecht (2000).

Green, M. D., "Characterisation of Suspensions in Settling and Compression," PhD Thesis, The University of Melbourne, Parkville, Australia (1997).

Green, M. D., and D. V. Boger, "Yield of Suspensions in Compression," *Ind. Eng. Chem. Res.*, **36**, 4984 (1997).

Green, M. D., M. Eberl, and K. A. Landman, "Compressive Yield Stress of Flocculated Suspensions: Determination via Experiment," *AIChE J.*, **42**, 2308 (1996).

Green, M. D., K. A. Landman, R. G. de Kretser, and D. V. Boger, "Pressure Filtration Technique for Complete Characterization of Consolidating Suspensions," *Ind. Eng. Chem. Res.*, **37**, 4152 (1998).

Hansen, P. C., "Analysis of Discrete Ill-Posed Problems by Means of the L-Curve," *SIAM Rev.*, **34**, 561 (1992).

Miller, K. T., R. M. Melant, and C. F. Zukoski, "Comparison of the Compressive Yield Response of Aggregated Suspensions: Pressure Filtration, Centrifugation and Osmotic Consolidation," *J. Amer. Ceram. Soc.*, **79**, 2545 (1996).

Shaw, W. T., and J. Tigg, *Applied Mathematica*, Addison-Wesley, Reading, MA (1994).

Weese, J., "A Reliable and Fast Method for the Solution of Fredholm Integral Equations of the First Kind Based on Tikhonov Regularization," *Comput. Phys. Commun.*, **69**, 99 (1992).

Manuscript received Jan. 18, 2001, and revision received June 1, 2001.